Available online www.jocpr.com

Journal of Chemical and Pharmaceutical Research, 2015, 7(7):1188-1193

Research Article

ISSN : 0975-7384
CODEN(USA) : JCPRC5

Spectroscopic properties of lanthanide and actinide triflates: Insight TDDFT

Meriem Lemmouchi and Nadia Ouddai

Laboratoire Chimie des matériaux et des vivants: Activité, Réactivité, Université- Hadj Lakhdar Batna- Algeria

---

ABSTRACT

Time-Dependent Density Functional Theory (TD-DFT) has become the most widely-used theoretical approach to simulate the optical properties. The TDDFT calculations of the lowest excited states of the lanthanide and actinide triflates $M(OTf)_n$; where (M= Ce, Th, Np, Pu, Am, Cm and Bk); (n=3 and 4) , provide an accurate description of their UV-visible spectra. The UV region is characterized by the most pointed and reduce peak of the $Th(OTf)_4$ compound that assigned to ligand metal charge transfer (LMCT) transition. The absorption specter of $Np(OTf)_3$ and $Pu(OTf)_3$ is mixed of LMCT, MLCT and intra charge transfer (ICT) transitions. The HOMO-LUMO transition of $Pu(OTf)_3$ are strongly bathochromically shifted compared with those of $Np(OTf)_3$ and $Th(OTf)_4$. These three complexes are capable to give a luminescence in the emission specter. The $M(OTf)_n$ where (M= Ce, Pu, Am, Cm and Bk); (n=3 and 4) are dominated in visible, ultra violet and infra read region by LMCT transition of the $Ce(OTf)_4$ and ICT of $Pu(OTf)_4$, $Am(OTf)_3$, $Cm(OTf)_3$ and $Bk(OTf)_3$.

Key words: TDDFT, Triflate, Lanthanide, Actinide, LMCT, MLCT, ICT

INTRODUCTION

The extension of Density functional theory (DFT) to the time dependent domain, namely time-dependent density functional theory (TDDFT) has been originally proposed by Runge and Gross 30 years ago.[1] Recently, the research of electroluminescent materials has been the subject of interest, and some researchers have extended their attention to heavy metal-coordinate complexes, even rare-earth complexes [2, 3]. Indeed, for such systems, the importance of excited-state-spin-contamination has been recently analyzed [4]. The TDDFT approach has been demonstrated to be reliable for calculating spectra properties of many transition metal complexes [5]. In this section we will focus on the spectroscopic properties of the lanthanide and actinide triflates complexes $M(OTf)_n$; where (M= Ce, Th, Np, Pu, Am, Cm and Bk); (n=3 and 4) , those used as Lewis acid catalysts in a variety of organic reactions, as well as precursors in inorganic and organometallic synthesis and they are also used in the nuclear industry [6].

EXPERIMENTAL SECTION

In this paper we carry out a quantum calculation on the lanthanide and actinide triflates $M(OTf)_n$; where (M= Ce, Th, Np, Pu, Am, Cm and Bk); (n=3 and 4); that coordinate with the OTf ligand as bidentate. The geometrical structures of the singlet ground state and the lowest lying triplet excited state are optimized by the DFT [7, 8] method with time-dependent functional theory approach TDDFT [9-12]/SAOP[13] calculations. All calculations are performed using the program ADF (Amsterdam Density Functional) developed by Baerends et al.[14] and the geometrical structures are fully optimized in gas state without any symmetry constraints.

RESULTS AND DISCUSSION

For all the triflate complexes $M(OTf)_n$; where (M= Ce, Th, Np, Pu, Am, Cm and Bk); (n=3 and 4), we have distinguished three categories appropriate to their range of wavelength.

3.1. The ultraviolet (UV) region:

This region is dominated by three triflate complexes such as the thorium, neptunium and plutonium triflates, with the general formula $Th(OTf)_4$, $Np(OTf)_3$ and $Pu(OTf)_3$ respectively.

The excitation energies E(ev), the wavelength λ (nm) and the greatest values of the oscillator strengths f are summarized in Tables 1. The tables also include the composition (%) of the excited states and the character of the transitions.

Table 1: The absorptions of the $Th(OTf)_4$, $Np(OTf)_3$ and $Pu(OTf)_3$ compounds according to TDDFT Calculations

Complex	λ (nm)	E(ev)	f	%	Transition	Character
$Pu(OTf)_3$	920.4958	1.3471	$0.5376\ e10^{-5}$	83	**HOMO → LUMO**	ICT
	332.1369	3.7334	$0.3064\ e10^{-2}$	98	**HOMO-4 → LUMO**	LMCT
	279.1786	4.4416	$0.1228\ e10^{-1}$	70	**HOMO-2 → LUMO+3**	ICT
	273.3083	4.5370	$0.6299\ e10^{-2}$	90	**HOMO-10→ LUMO**	LMCT
	271.210	4.5721	$0.1225\ e10^{-2}$	85	**HOMO-3 → LUMO+12**	MLCT
	266.0373	4.6610	$0.2986\ e10^{-2}$	95	**HOMO-10 → LUMO+1**	LMCT
$Th(OTf)_4$	252.8187	4.9047	$0.3422\ e10^{-6}$	100	**HOMO → LUMO**	LMCT
	231.416	5.3583	$0.1099\ e10^{-1}$	78	**HOMO- 4 → LUMO+1**	LMCT
	228.811	5.4193	$0.1726\ e10^{-1}$	67	**HOMO → LUMO+5**	LMCT
	226.7532	5.4685	$0.3799\ e10^{-2}$	95	**HOMO-6 → LUMO+3**	LMCT
	214.1438	5.7905	$0.5787\ e10^{-2}$	97	**HOMO- 3 → LUMO+5**	LMCT
	211.7739	5.8553	$0.2093\ e10^{-2}$	98	**HOMO- 6 → LUMO+6**	LMCT
$Np(OTf)_3$	624.811	1.9846	$0.4607\ e10^{-6}$	4	**HOMO → LUMO**	ICT
	332.4664	3.7297	$0.1779\ e10^{-1}$	61	**HOMO-2 → LUMO+11**	ICT
	330.1911	3.7554	$0.1675\ e10^{-1}$	68	**HOMO- 2 → LUMO+12**	MLCT
	265.0648	4.6781	$0.1099\ e10^{-1}$	67	**HOMO → LUMO+11**	ICT
	246.766	5.0250	$0.8501\ e10^{-2}$	99	**HOMO- 3 →LUMO+1**	LMCT
	237.789	5.2145	$0.3903\ e10^{-2}$	31	**HOMO- 5 → LUMO**	LMCT

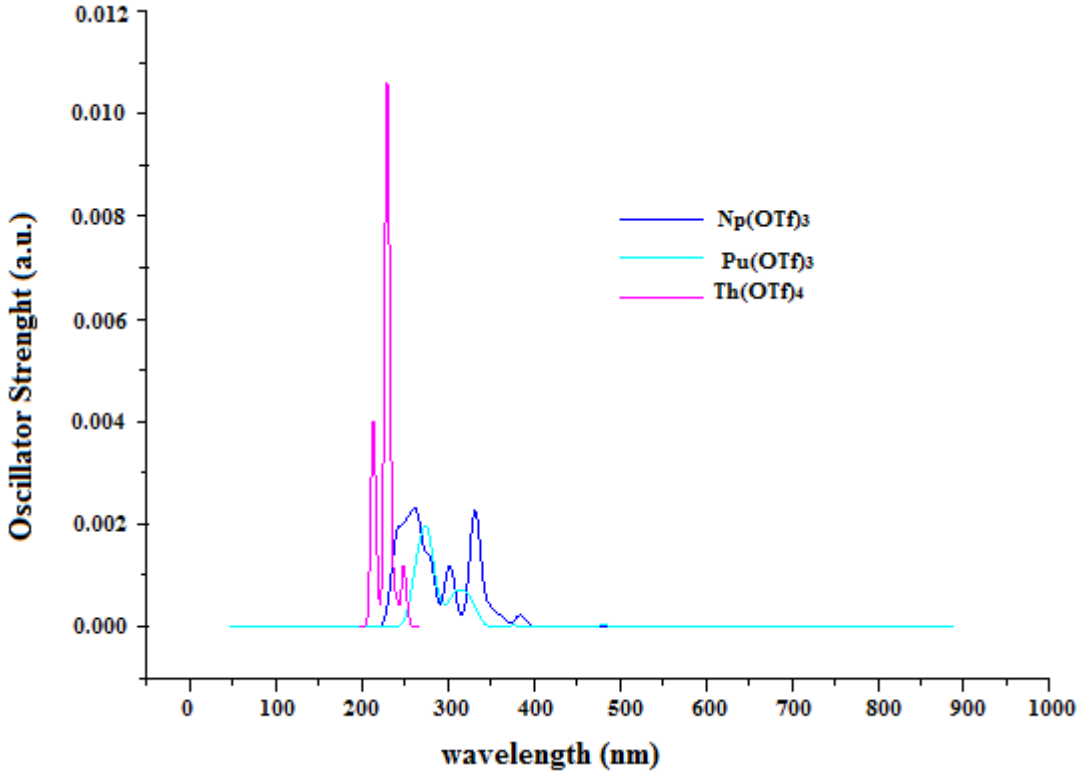

Figure1: Theoretical UV absorption spectra of $Np(OTf)_3$, $Pu(OTf)_3$ and $Th(OTf)_4$ complexes

The absorption spectra reported in Figure 1 are dominated in the UV regions by absorption features which are given in Table1. The specter of $Th(OTf)_4$ is reduced comparing with those of $Np(OTf)_3$ and $Pu(OTf)_3$ (see Figure 1), and it has the most pointed peak that assigned to LMTC transition (ligand to metal charge transfer). A blend of transition character is observed in the case of $Np(OTf)_3$ and $Pu(OTf)_3$: MLCT, ICT and LMCT [15- 18].

The main difference in the absorption spectra of these three compounds is that HOMO-LUMO transition of $Pu(OTf)_3$ are strongly bathochromically shifted compared with those of $Np(OTf)_3$ and $Th(OTf)_4$. These three complexes are capable to give a luminescence in the emission (see Table 1).

The frontier orbitals relevant to discussion are available as supporting information. In both of the $Pu(OTf)_3$ and the $Np(OTf)_3$ complexes, the HOMO's and LUMO's are nearly completely localized between the metal and the ligand OTf, while in the case of the $Th(OTf)_4$ complex, the HOMO's and LUMO's are localized on the OTf ligand and the thorium metal respectively. The important transitions of these three complexes are shown in Figure 2.

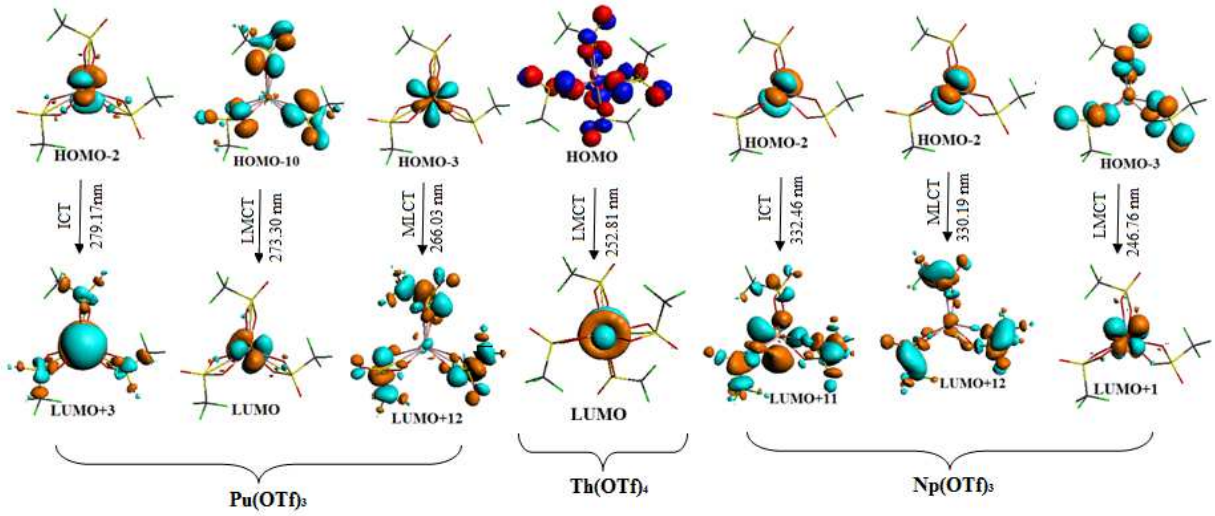

Figure2: The excitation transitions for the $Pu(OTf)_3$, $Th(OTf)_4$ and $Np(OTf)_3$ calculated by TD-DFT in gas phase

3.2. The visible region:

In the visible domain, there are two dominated complexes the cerium triflate $Ce(OTf)_4$ and the plutonium triflate $Pu(OTf)_4$. The electronic absorption spectra of these complexes are shown in Table 2.

For the $Pu(OTf)_4$, a relatively broad band centered in all complexes at 615 nm, 517 nm, 480 nm, 452 nm and 437 nm . The visible region of $Ce(OTf)_4$ is characterized by a rather intense band between 493 nm and 424 nm (see Figure 4).

On the basis of the calculated excitation energies and oscillator strengths, the $Ce(OTf)_4$ complex is the best candidate with a quite intense feature peaking comparing to the $Pu(OTf)_4$ at about 452 nm (see Table 2 and Figure 4), this feature has a clear LMCT character (see Figure 3).

Table 2: The absorptions of the $Ce(OTf)_4$ and $Pu(OTf)_4$ compounds according to TDDFT Calculations

Complex	λ (nm)	E(ev)	f	%	Transition	Character
$Ce(OTf)_4$	493	2.5144	$0.2236\ e10^{-4}$	53	**HOMO → LUMO**	LMCT
	461	2.6889	$0.1723\ e10^{-2}$	35	**HOMO- 1 → LUMO+3**	LMCT
	459	2.7003	$0.3686\ e10^{-2}$	37	**HOMO- 5 → LUMO**	LMCT
	437	2.8374	$0.1615\ e10^{-1}$	54	**HOMO- 1 → LUMO+6**	LMCT
	426	2.9116	$0.1959\ e10^{-1}$	46	**HOMO- 4→ LUMO+6**	LMCT
	424	2.9236	$0.1454\ e10^{-1}$	58	**HOMO-5 → LUMO+6**	LMCT
$Pu(OTf)_4$	872	1.4220	$0.4570\ e10^{-4}$	52	**HOMO → LUMO**	ICT
	615	2.0163	$0.2376\ e10^{-2}$	49	**HOMO-2 → LUMO+1**	ICT
	517	2.3995	$0.2392\ e10^{-2}$	63	**HOMO-3 → LUMO+1**	ICT
	480	2.5849	$0.4019\ e10^{-2}$	52	**HOMO-8→ LUMO+1**	ICT
	452	2.7432	$0.1072\ e10^{-1}$	57	**HOMO-7→ LUMO+2**	ICT
	437	2.8374	$0.1105\ e10^{-1}$	20	**HOMO-3 → LUMO+3**	ICT

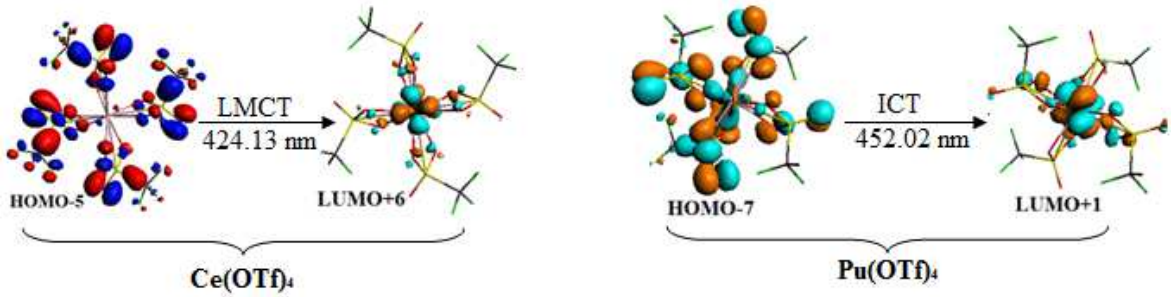

Figure3: The excitation transitions for the $Pu(OTf)_4$ and $Ce(OTf)_4$ calculated by TD-DFT in gas phase

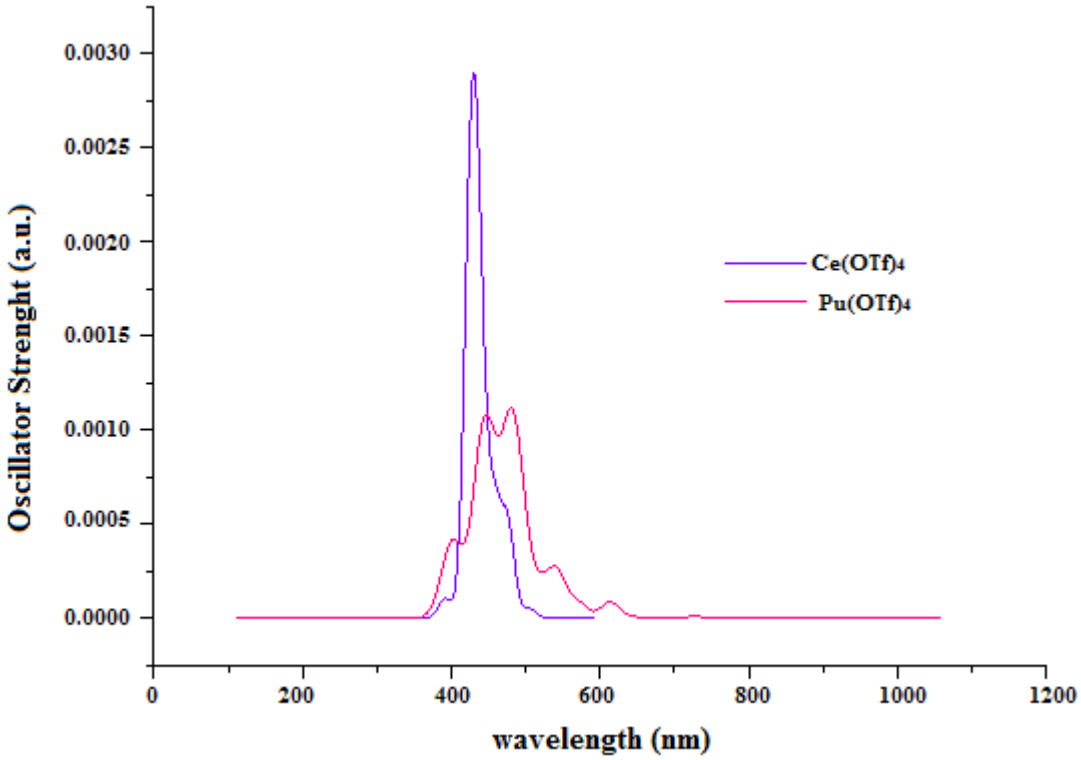

Figure4: Theoretical UV absorption spectra of $Np(OTf)_3$, $Pu(OTf)_3$ and $Th(OTf)_4$ complexes

Table 3: The absorptions of the $Am(OTf)_3$, $Bk(OTf)_3$ and $Cm(OTf)_4$ complexes according to TDDFT Calculations

Complex	λ (nm)	E (ev)	f	%	Transition	Character
$Am(OTf)_3$	1056	1.1739	$0.5175\ e10^{-3}$	46	**HOMO → LUMO**	ICT
	483	2.5682	$0.6641e10^{-2}$	68	**HOMO-5 → LUMO**	ICT
	423	2.9343	$0.2131\ e10^{-2}$	39	**HOMO-10 →LUMO**	ICT
	377	3.2894	$0.1169\ e10^{-2}$	83	**HOMO-11 →LUMO**	ICT
	302	4.1065	$0.9679\ e10^{-2}$	86	**HOMO-12 → LUMO+1**	ICT
	278	4.4676	$0.1639\ e10^{-2}$	92	**HOMO-20 → LUMO**	ICT
$Cm(OTf)_3$	824	1.5055	$0.3674\ e10^{-2}$	18	**HOMO → LUMO**	ICT
	518	2.3919	$0.1424\ e10^{-1}$	39	**HOMO-5 → HOMO-4**	ICT
	496	2.4987	$0.1002\ e10^{-1}$	26	**HOMO-9 → LUMO**	ICT
	396	3.1334	$0.1678\ e10^{-1}$	69	**HOMO- 16 →LUMO**	ICT
	279	4.4438	$0.9150\ e10^{-2}$	99	**HOMO-5 → LUMO+1**	ICT
	232	5.3492	$0.3294\ e10^{-2}$	62	**HOMO-6 → HOMO**	ICT
$Bk(OTf)_3$	678	1.8286	$0.1341\ e10^{-2}$	50	**HOMO → LUMO**	ICT
	624	1.9874	$0.1341\ e10^{-2}$	57	**HOMO-1 → LUMO+4**	ICT
	581	2.1355	$0.1503\ e10^{-1}$	31	**HOMO-4 → LUMO+4**	ICT
	421	2.9452	$0.1125\ e10^{-1}$	80	**HOMO-12 →LUMO+4**	ICT
	314	3.9458	$0.6701\ e10^{-2}$	38	**HOMO-2 →LUMO+2**	ICT
	273	4.5349	$0.2530\ e10^{-2}$	74	**HOMO-9 →LUMO+1**	ICT

3.3. The UV-Visible- IR region

The absorption spectra reported in Figure 5 are dominated in the UV-Visible- IR region by absorption features which are given in Table 3. The main difference in the absorption spectra of the three compounds $Am(OTf)_3$, $Cm(OTf)_3$ and $Bk(OTf)_3$ is that all ICT transitions and they are strongly bathochromically shifted compared with those studied previously.

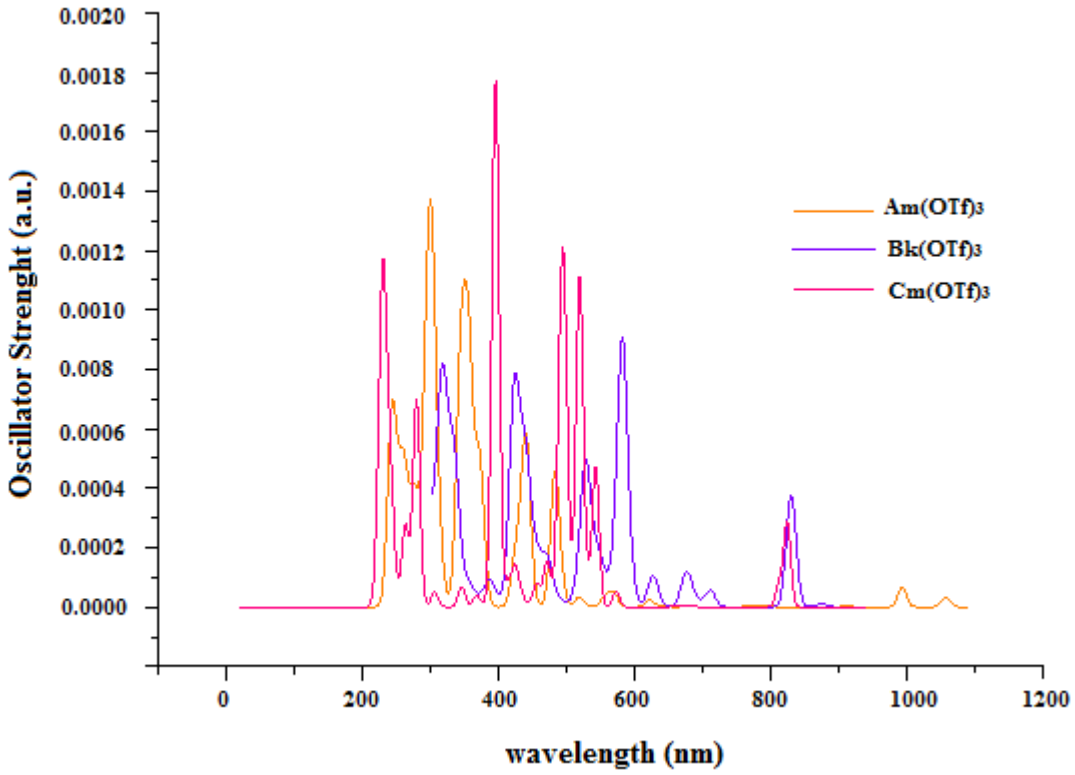

Figure5: Theoretical UV absorption spectra of $Am(OTf)_3$, $Bk(OTf)_3$ and $Cm(OTf)_4$ complexes

CONCLUSION

In this paper, we have applied the TDDFT methods to investigate the absorptions and luminescence properties of the lanthanide and actinide triflates complexes $M(OTf)_n$; where (M= Ce, Th, Np, Pu, Am, Cm and Bk); (n=3 and 4). The calculated results reveal that the $Th(OTf)_4$, $Np(OTf)_3$ and $Pu(OTf)_3$ complexes are dominated in UV region, with small values of the oscillator strengths f in the HOMO – LUMO's transitions. The ligand to metal charge transfer LMCT is the predominated character in the case of the $Th(OTf)_4$ and a combination of LMCT , MLCT and ICT is observed in the case of $Np(OTf)_3$ and $Pu(OTf)_3$ complexes. The domination in UV region probably allows to these complexes to show luminescence in the emission specter. In the case of the $Pu(OTf)_4$, $Am(OTf)_3$, $Cm(OTf)_3$ and $Bk(OTf)_3$ compounds, the transitions are intramolecular charge transfer ICT. The visible region of the $Ce(OTf)_4$ is characterized by a rather intense band between 493 nm and 424 nm and LMCT transition character.

REFERENCES

[1] E Runge; EKU Gross, Phys. Rev. Lett., **1984**, 52, 997.
[2] (a) JF Wang; RY Wang; J Yang; ZP Zheng; MD Carducci; T. Cayou; N Peyghambarian; GE Jabbour, J. Am. Chem. Soc., **2001**, 123, 6179.
(b) V Christou; OV Salata; TQ Ly; S Capecchi; N J Bailey; A Cowley ; AM Chippindale, Synth. Met., **2000** , 7, 111-112.
(c) S Eliseeva; O Kotova; O Mirzov; K Anikin; L Lepnev; E Perevedentseva; A Vitukhnovsky; N Kuzmina, Synth. Met., **2004** ,141, 225.
(d) YK Kim; SW Pyo; DS Choi; HS Hue; SH Lee; YK Ha; HS Lee; JS Kim ; WY Kim, Synth. Met., **2000**, 113, 111-112.
(e) H Xin; FY. Li; Mei Shi; ZQ Bian; CH Huang, J. Am. Chem. Soc., **2003**, 125, 7166.
[3] (a) SF Li; GY Zhong; WH Zhu; FYJF Li; W Pan; H. Tian, J. Mater. Chem., **2005**, 15, 3221.

(b) PP Sun; JP Duan; HT Shih; CH Cheng, Appl. Phys. Lett., **2002**, 81, 792.
(c) JB Yu; L Zhou; HJ Zhang; YX Zheng; HR Li; RP Deng; ZP Peng ; ZF Li, Inorg. Chem., **2005**, 44, 1611.
(d) C Adachi; MA Baldo; SR Forrest, J. Appl. Phys., **2000**, 87, 8049.
[4] A Ipatov; F Cordova; LJ Doriol; ME Casida, J. Mol. Struct.: THEOCHEM., **2009**, 914, 60.
[5] (a) T Liu; HX Zhang; BH Xia, J. Phys. Chem. A., **2007**, 111, 8724.
(b) X Zhou; HX Zhang; QJ Pan; BH Xia; AC Tang, J. Phys. Chem. A., **2005**, 109, 8809.
(c) X Zhou; AM Ren; Feng, J. K. J. Organomet. Chem., **2005**, 690, 338.
(d) A Albertino; C Garino; S Ghiani; R Gobetto; C Nervi; L Salassa; E Rosenverg; A Sharmin; G Viscardi; R Buscaino; G Cross; MJ Milanesio, Organomet. Chem., **2007**, 692, 1377.
[6] GA Lawrance, Chem. Rev., **1986**, 17, 86.
[7] A Becke, Phys. ReV., **1988**, A 38, 3098.
[8] JP Perdew. Phys. ReV. B. 33., **1986**, 8822.
[9] EKU Gross; W Kohn, AdV. Quantum Chem., **1990** , 21, 255.
[10] EUK Gross; JF Dobson; M Petersilka, Density Functional Theory. In Springer Series "Topics in Current Chemistry", Nalewajski, R F Ed, Springer: Heidelberg., **1996**.
[11] ME Casida, In Recent Advances in Density Functional Methods, Chong, D P Ed, World Scientific: Singapore., **1995**, 155.
[12] R Bauernschmitt; R Ahlrichs, J. Chem. Phys., **1996**, 104, 9047.
[13] A Rosa; G Ricciardi, unpublished results.
[14] EJ Baerends; DE Ellis; P Ros, Chem. Phys., 1973, 2, 41.
[15] CS Kramer; TJJ Muller, Eur. J. Org. Chem., **2003**, 18, 3534.
[16] (a) AP Kulkarni; PT. Wu; TW Kwon; SA. Jenekhe, J. Phys. Chem., **2005**, 109, 19584.
(b) M Sailer; M Nonnenmacher; T Oeser; TJ Muller, J. Org. Chem. **2006**, 423.
[17] (a) RY Lai; EFL Fabrizio; SA Jenekhe; AJ Brd, J. Am. Chem. Soc., **2001**, 123, 9112.
(b) RY Lai; X Kong; SA Jenekhe ; AJ Bard, J. Am. Chem. Soc., **2003**, 125, 12631.
[18] M Kurosawa; T Nankawa; T Matsuda; K Kubo; M Kurihara; H Nishihara, Inorg. Chem., **1999**, 38, 5113.